

Interactive Rendering of Complex 3D-Treemaps With a Comparative Performance Evaluation

Matthias Trapp, Sebastian Schmechel, Jürgen Döllner

Hasso-Plattner-Institut, University of Potsdam, Germany

{matthias.trapp, sebastian.schmechel, juergen.doellner}@hpi.uni-potsdam.de

Keywords: 3D-treemaps, real-time rendering, performance evaluation

Abstract: 3D-Treemaps are an important visualization technique for hierarchical views. In contrast to 2D-Treemaps, height can be used to map one additional attribute of the data items. Using the Treemap technique in combination with large datasets (more than 500k) a fast rendering and interaction techniques that are beyond collapsing/uncollapsing nodes is still one of the main challenges. This paper presents a novel rendering technique that enables the image synthesis of geometrical complex 3D-Treemaps in real-time. The fully hardware accelerated approach is based on shape generation using geometry shaders. This approach offers increased rendering performance and low update latency compared to existing techniques and through it enables new real-time interaction techniques to large datasets.

1 INTRODUCTION

Motivation The concept of treemaps is an important tool for visualization of large hierarchical datasets. Its extension to the third dimension enables a number of applications, like metaphor-based visualization that support the user’s mental model creation of abstract datasets and through it the memorability of items as shown in InformationPyramids (Andrews et al., 1997) and CodeCity (Wettel and Lanza, 2008). However, the additional dimension comes with additional concerning the geometric representation and image-synthesis. In particular, this introduces challenges for the interactive rendering of complex 3D-Treemaps. Complex 3D-Treemaps are described by a large number of treemap items, e.g., more than 500k (Fig. 1), and diverse attribute mappings to color and height of these items.

Basically the interaction in 3D-Treemaps can be grouped in three main tasks: (a) Navigational tasks (e.g., Zooming and Panning), (b) Explorational tasks (e.g., implicit and explicit visualization of nodes attributes and informations), and (c) Data-Modification tasks (adding or removing nodes). While navigation and exploration tasks are independent from the complexity of the underlying layout algorithm, Data-Modification tasks result in a recomputation of the layout. Nevertheless the degree of user experience for layout-independent tasks are highly connected to the rendering run-time (Correa et al., 2003). Bladh

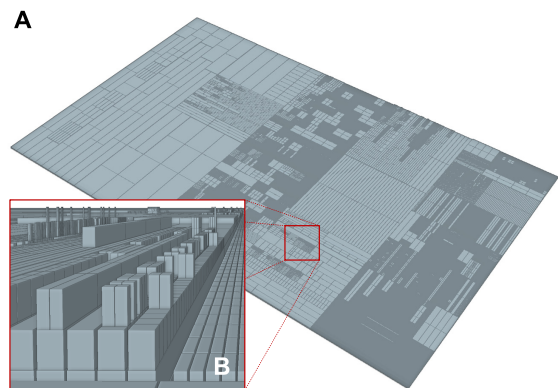


Figure 1: An example of a complex 3D-Treemap with 614k items rendered with the presented shape generation approach in real-time. It comprises over six million rendering primitives.

et al. present a visualization techniques that support interactive (real-time) image synthesis and allow navigation and exploration tasks through animated transitions (Bladh et al., 2005). In addition to that, a change or update of mappings on rendered treemap artifacts, require a high update performance.

Rendering of Complex 3D Scenes To summarize, despite the performance of the layout algorithm and dynamic update of treemaps, the efficient rendering remains a challenge. The efficient interactive render-

ing of complex 3D-Treemaps depends on the following three aspects concerning the rendering techniques as well as the underlying data representation:

Rendering Performance The run-time complexity for the rendering of a single frame must be small enough to support interactive frame rates for a high number of treemap items. The rendering performance often depends on the geometric representation of the datasets.

Update Performance The update performance is determined by the number of changes in treemap representation required for a specific visualization. Thus, increasing the update performance contributes to the available per-frame rendering budget.

Memory Consumptions The memory consumptions (both in main and video memory) of a 3D-Treemap representation determines the maximum amount of 3D-Treemap items that can be rendered without using out-of-core mechanisms, which introduce additional IO operations and more complex implementations. Therefore, the space complexity of a representation should be as compact as possible.

Thus, the main goals of a rendering technique that facilitate the interactive rendering of complex 3D-Treemaps are the reduction of rendering, update, and storage costs.

Contributions Concerning the challenges stated above, this paper presents a novel, fully hardware-accelerated rendering technique that is capable of performing real-time image-synthesis for complex 3D-Treemaps within a single rendering pass. The approach is based on *server-side shape generation*, i.e., the geometry of 3D-Treemap items is created on graphics hardware. This reduces bandwidth and increases uptime performance, as well as enables a compact representation of a 3D-Treemap with a minimal memory footprint. Its implementation is based on OpenGL and the OpenGL Shading Language (Segal and Akeley, 2012); an API which is of broad use within scientific visualization. The presented concepts can also be transferred to D3D compatible applications. To summarize, this paper makes the following contributions to the community:

1. Presents a novel rendering technique especially suitable for rendering complex 3D-Treemaps in real-time. This technique is especially suitable for interaction metaphors without recomputing the treemap layout.

2. Describes the implementation of different concurrent rendering techniques for the interactive rendering of complex 3D-Treemaps.
3. Evaluates and compares these rendering techniques with respect to rendering performance, update performance, and memory consumptions.

The remainder of this paper is structured as follows. Section 2 reviews related and previous work with respect to 3D-Treemaps and rendering approaches. Section 3 describes the shape generation approach and existing techniques suitable for the interactive rendering of complex for 3D-Treemaps. Section 4 gives implementation details. Section 5 presents a performance analysis and comparison of the rendering techniques. Finally, Section 6 concludes the paper.

2 RELATED WORK

Treemaps are a common used technique for space-restricted visualization in the last two decades. The original algorithm presented by Shneiderman recursively splits parent nodes alternating in horizontal and vertical direction by their child nodes (Shneiderman, 1992). One major disadvantage of the Slice'n Dice algorithm is the creation of unfavorable aspect ratios of the node representations. Bruels et al. as well as Bederson and Shneiderman counter the problem with Squarified- (Bruels et al., 2000) and Strip-Treemap (Bederson et al., 2002) layouts. Fekete and Plaisant use treemaps to visualize datasets with about one million nodes. In addition to visualize the structure of the hierarchy, the items' attributes were also visualized by mappings onto size and color (Fekete and Plaisant, 2002). The increasing number of items in large hierarchies leads to perceptual questions about Treemap visualizations, e.g., how much effect does the width of a nodes' border have on the ability to extract the hierarchical structure of the underlying data (Kong et al., 2010).

The first extension of 2D-Treemap layout algorithms to the third dimension are presented in the StepTree by Bladh et al.. They extend the initial algorithm by stacking the graphical representations of subdirectories on top of its parent's one (Bladh et al., 2004). In a comparative study between the StepTree and its corresponding 2D-Treemap users significantly performed better in tasks of interpreting the hierarchical structure, while preserving performance in other interpretational and navigational tasks. Wettel and Lanza use 3D-Treemaps to create a metaphorical view on software system artifact hierarchies with CodeCities (Wettel and Lanza, 2008)

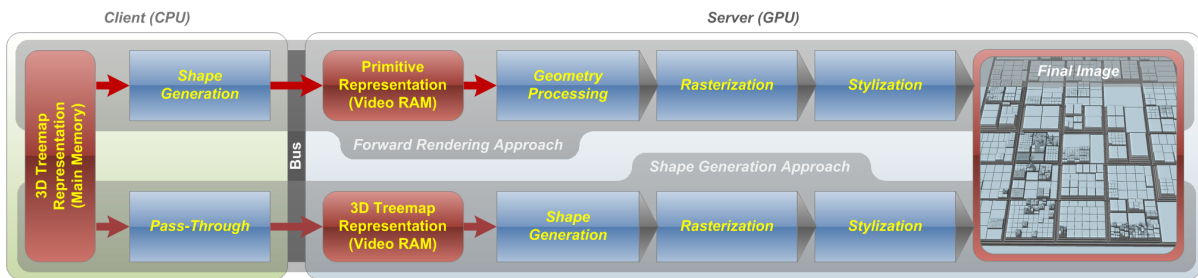


Figure 2: Comparison of different rendering pipelines for client-side (CPU) shape generation (top) and our server-side shape generation (bottom).

by mapping additional information to the height of leaf nodes. This leads to a treemap-based layout with graphical representations of software system artifacts as high and low “buildings” grouped in areas of the “software city”. Several other publications address the use of 3D-Treemaps in Software Visualization in depth (Liggesmeyer et al., 2009; Bohnet and Döllner, 2011). Bohnet and Döllner also mentioned that the use of realistic rendering effects, e.g., shadowing, in 3D-Treemaps support the users’ perception of the elements as distinguished ones (Bohnet and Döllner, 2011). All of the aforementioned publications use 3D-Treemaps by extruding the nodes, calculated with a 2D-layout algorithm, by one additional attribute mapping. In addition to this classical approach there exist a variety of modifications and extensions, e.g., 3D-Polar Treemaps, Treecube or Collector’s Box Treemap (Schulz et al., 2011), one can categorize by four attributes (a) containment relationship, (b) used graphics primitives, (c) layout method and (d) alignment (Schulz et al., 2007).

Even though the visualization of a wide range of large hierarchical datasets, e.g., software systems, economy data, is frequently studied, the interaction techniques used in this field are straightforward. Appearing techniques in 3D-Treemaps are the selection of nodes and leafs, as well as the coloring/highlighting of nodes (Wettel and Lanza, 2008). Sud et al. present a solution to provide interactive rendering, navigation and animation of dynamically changing 2D-Voronoi-Treemaps by using a GPGPU-based rendering technique (Sud et al., 2010).

With an increasing amount of nodes the geometrical complexity of treemap grows directly, resulting in the need of general computer graphical techniques to create an interactive visualization. One way to achieve a lower memory footprint and a faster rendering is the algorithm for triangle strip optimization shown by Evans et al. (Evans et al., 1996).

3 RENDERING TECHNIQUES

The rendering techniques in this paper is a combination of standard forward rendering and deferred shading (Liktor and Dachsbacher, 2012). Despite intermediate rendering (also known as the obsolete intermediate mode in former OpenGL specifications), three types of techniques are suitable for the interactive rendering of complex 3D-Treemaps: (1) using (indexed and non-indexed) vertex buffer objects (Section 3.3), geometry instancing variants (Section 3.4), as well as a novel server-side shape generation approach (Section 3.2).

For clarification, Figure 2 shows a comparison of the different, simplified pipelines suitable for rendering geometrical complex 3D-Treemaps. The illustration on top shows classical forward rendering pipeline as used for the existing rendering approaches. The geometry required for the rendering of 3D-Treemaps is generated on the client side (CPU). This implies the generated geometry must be transferred to server every time the representation changes, e.g., due to changes in the layout or in the thematic mapping. We denote this pipeline model as *client-side shape generation*. In contrast thereto, the illustration on the bottom shows the rendering pipeline for the presented *server-side shape generation*. The advantage of this approach lies in the deferred shape generation on the graphics board (GPU) for only items that are visible in the current view frustum.

3.1 Preliminaries

All rendering techniques make the following assumptions on the structure and visualization of a 3D-Treemap. A 3D-Treemap can be considered as a special case of 2.5D virtual environment. Such VE is usually not viewed from below, thus, we do not consider the bottom faces of a treemap item important.

Further, for the simplification of the geometric representation, it is assumed that 3D-Treemap items are aligned with world space coordinate axis. Furthermore, we assume that attributes for thematic map-

pings vary usually per treemap item as well as that thematic mappings vary more often than the layout of a 3D-Treemap changes.

Layout & Thematic Mapping There are several layout approaches for 2D-Treemaps (e.g., squarified (Bruls et al., 2000) or strip layouts (Bederson et al., 2002)). For simple 3D-Treemaps the layout costs are usually higher than the rendering costs. Since, 3D-Treemaps are basically 2D-treemaps with an additional height value per item, existing layout approaches can be used. Thus, the *layout-dependent attributes* of a 3D-Treemap item are 2D position (horizontal and vertical) and 2D dimensions (width and height).

However, changes in the layout caused by modification of the underlying data can be separated from changes in the visual appearance due to altering thematic mappings (*layout-independent attributes*): both can occur at different frequencies. Consequently, but depending on the respective applications, one can assume that separate handling of layout-dependent and layout-independent attributes has influence on the update performance and thus, the rendering performance.

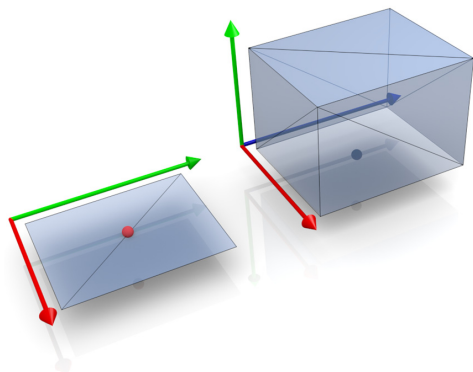


Figure 3: Comparison of the geometric representation for a 2D (left) and a 3D-treemap item (right).

3D-Treemap Items The additional dimension introduces additional geometric complexity, i.e., geometric primitives. A 3D-Treemap item requires three to five (depending on the use of backface-culling) times more geometry than a 2D equivalent. In contrast to 2D-Voronoi-Treemaps (Balzer and Deussen, 2005), classical 2D-Treemaps (Bruls et al., 2000) have a squared footprint that can be geometrically represents using two triangles (Fig. 3 left). Extending the 2D-Treemap concept to the third dimension introduces at minimum five times more geometric primitives (Fig. 3 (right)).

For complex 3D-Treemaps an important goal is to provide a minimal representation, with a small-as-possible memory footprint on client. The size of the item representation determines the update performance. Further, memory alignment should support fast client-server updates.

In contrast, to Voronio or circular treemap elements, a standard treemap item is represented using a 3D box. A treemap item T of a treemap \mathcal{T} can be expressed as: $T = (P, D, C, id, F)$. The position $P = (x, y, z) \in \mathbb{R}^3$ represents the origin of the cube, the extends by dimension $D = (w, h, d) \in \mathbb{R}^3$, the color $C \in [0, 1] \subset \mathbb{R}^3$. In addition thereto, a treemap item can store a number of flags F , describing properties such as the hierarchy depth or if it is a leaf node. The unique object identifier id enables the usage of indirections during rendering, i.e., if attributes changes: no geometry update is required.

Based on the previous layout assumptions, the presented concept uses two buffers that can be updated separately to save bandwidth and update time for animated treemaps (Section 4). One buffer represents the static layout-dependent information (i.e., x, y, w, h) while the other one contains the information about possibly dynamic, layout-independent properties (i.e., z, d, C).

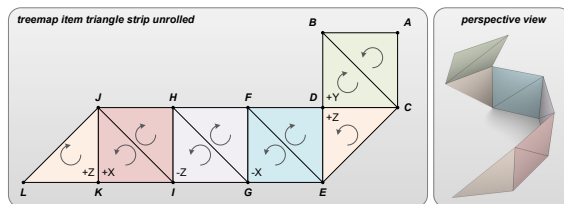


Figure 5: Example of a primitive template: triangle strip for representing a 3D-Treemap item on GPU.

Compact Representation The major goal is to provide a compact representation of the 3D-Treemap that is suitable for client and server storage by conveying high frame rates at the same time. Figure 5 shows the used geometry template for an indexed representation for a cube without a bottom face. It only requires 8 vertices and 12 indices to describe ten faces. To summarize, the compact representation also enables a lossless compression for 3D tree maps. For example, Table 1 compares the memory footprints for n treemap items described by the number a of 32bit floating point attributes, with a 4 Byte representation of each one. It achieves a compression ratio of 1:2.5 over indexed vertex representations and a ratio of 1:3.75 over non-indexed vertex representations. This form of lossless compressed representation can especially be applied for transferring geometric data using the world wide web. It can become especially

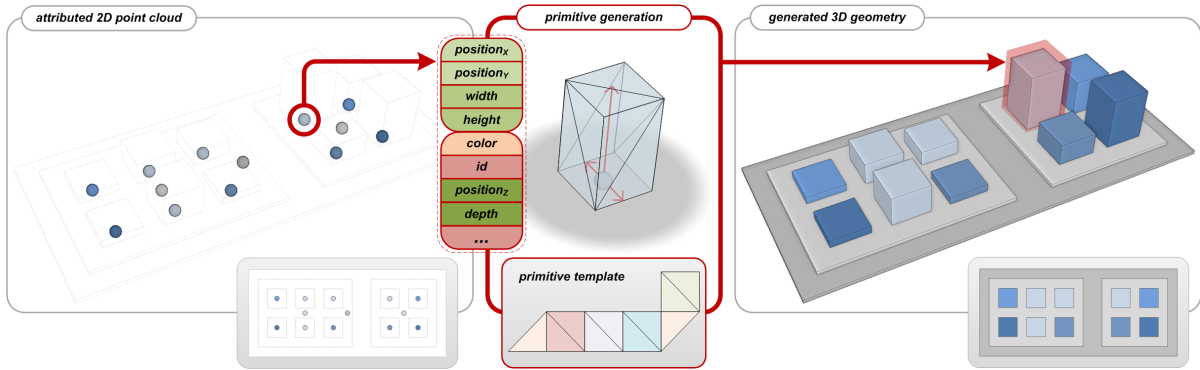


Figure 4: Simplified rendering pipeline for the shape generation approach presented in this paper. An attributed point cloud is converted to cubes using a primitive template in the geometry shader stage. The insets shows the test datasets from a 2D perspective.

suitable for client-side rendering using WebGL, if geometry shader functionality will be supported in future specifications.

3.2 Shape Generation Approach

This fully GPU accelerated, single-pass rendering approach is based on the idea of *Instance Culling* or *Instance Cloud Reduction* (Rákos, 2010), which originally comprises a culling pass and a rendering pass. We modify the concept by omitting the culling pass and by shifting the geometric representation and the assembly of each geometric instance completely to the geometry shader.

Figure 4 shows an simplified overview of the rendering pipeline for the proposed shape generation approach. Buffer objects encode all items as attributed point cloud. The point position is the origin of the 3D-Treemap item. During a single draw call, a geometry shader converts a input point into a triangle strip, representing the shape of the 3D-Treemap item, using the indexed primitive template described in the previous section.

Table 1: Comparing memory footprints of the rendering techniques on VRAM in Byte.

Rendering Technique	Memory Footprint
Shape Generation	$n \cdot (a \cdot 8) + 24 + 12$
Indexed VBO	$n \cdot (a \cdot 8 + 12)$
Non-Index VBO	$n \cdot (a \cdot 30)$
Pseudo Instancing	$8 + 12$
UBO Instancing	$n \cdot (a \cdot 8) + 24 + 12$
TBO Instancing	$n \cdot (a \cdot 8) + 24 + 12$

3.3 Vertex Buffer Approaches

An alternative to the shape generation approach is the rendering using server-side resources known as *buffer objects*. Buffer objects is the general term for unformatted linear memory, allocated by the graphics context (Segal and Akeley, 2012). These can be used to store vertex data. For comparison reasons, two GPU representation variants for 3D-Treemaps are evaluated:

Indexed Buffer Objects Indexing, or indexed vertex rendering, enables the reuse of vertices by using an additional index buffer. In this way, a treemap item can be represented using eight vertices and 12 indices (Fig. 5). Indexed vertex rendering also leverage the GPU’s post-transform cache (post-T&L cache) (ca. 32 vertices) that reuses already transformed vertices (Hoppe, 1999).

Non-Indexed Buffer Objects For reasons of completeness, we compare the shape generation approach with the non-indexed buffer object representation. Here, a treemap item is represented using ten faces with three vertices. The representation does not utilize post-transform cache and has the largest video memory footprint of all compared rendering techniques.

In contrast to shape generation, such explicit buffer representation exhibit higher memory consumptions and increased update-time per treemap item, since the shape generation is performed client side for the compact treemap representation described in Section 3.1.

3.4 Geometry Instancing

Another important technique for the interactive rendering of uniform geometry is *geometry instancing*

(Nguyen, 2007). It enables the rendering of a number of copies (instances) of a single geometric object in a single draw call and thereby improves the potential runtime performance. This technique is primarily used for objects such as trees (Bao et al., 2011), grass, buildings, or objects which can be in general represented as repeated geometry. Although vertex data is duplicated across all instanced meshes, each instance can have differentiating parameters (per-instance data). This paper evaluates three common instancing techniques that mainly differ by the encoding of *per-instance data* such as dimension, color, and object identifier.

Pseudo Instancing encodes the instance data in the *shader constant registers*. These registers are usually limited to 4k of floating point values. Pseudo instancing requires most draw calls because of the limited number of instances that can be represented.

Uniform-Buffer Instancing stores instance data in uniform buffer objects (UBO) (often with a maximum buffer size of 64k). The maximal size of a uniform buffer determines number of instances rendered with a single draw call, i.e., the number of draw calls required to render the complete treemap.

Texture-Buffer Instancing uses so called *texture buffer objects* (TBO) that provide a 1D storage as a texture. Similar, to uniform-buffer instancing, the maximum size of a texture buffer determines number of draw call. The instance data is accessed using texel fetches during shader runtime. The number of item attributes determines the number of texel fetches required.

For a test machine equipped with a NVIDIA GTX 460, a 3D-Treemap data comprising 614,929 items the per-instance data require 29,516,592 byte. Pseudo instancing requires 1809 draw calls with 340 instance per call, while uniform buffer instancing requires 453 draw calls with 1360 instances per call. Since buffer textures can be substantially larger than equivalent one-dimensional textures (up to 2^{27} texels), texture buffer instancing requires only a single draw call. The performance impact of each technique is discussed detailed in Section 5.

3.5 Culling Optimizations

The implementation of the rendering techniques described above support the following three culling techniques to improve rendering performance:

View-Frustum Culling View-frustum culling performed in the vertex stage is used to omit the

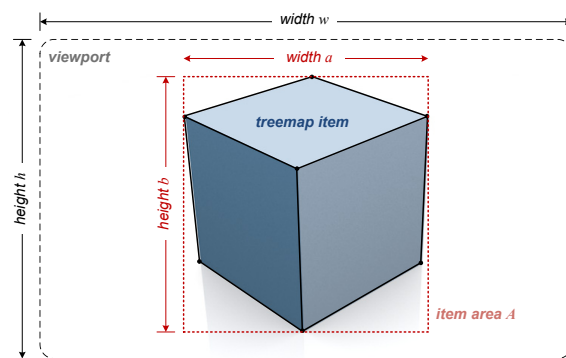


Figure 6: Parameters in screen-space coordinates required for size culling a 3D-Treemap item.

shape generation for treemap items outside the current view frustum. A two-stage approach is applied: first; test only the origin point, if it is outside the current view frustum, each one of the eight corner points are tested.

Size-Culling If a 3D-Treemap item passes view-frustum culling, the area of its projected shape in screen space is tested. No geometry is emitted if the size is below a threshold. This reduces rasterization costs.

Back-Face Culling To further reduce rasterization costs, back-face culling is enabled for 3D scenes with opaque geometry.

The application of occlusion culling is not considered due to the low geometric complexity of the 3D-Treemap items, i.e., simple approximations of treemap geometry have the same complexity, thus occlusion culling wont give any benefits. Further, user mainly look from top-down or oblique perspectives, thus, most items are visible and not overdrawn.

The size culling approach omits the rasterization of treemap items which dimensions are too small to be perceived on screen. This can significantly reduces the load of the rasterization stage in the rendering pipeline. We propose a screen-space metric in combination with a threshold $\epsilon > 1$ over the item area A of a projected treemap item (Figure 6):

$$passSizeCulling(a, b, \epsilon) = \begin{cases} 1 & a \cdot b > \epsilon \\ 0 & otherwise \end{cases}$$

The area A computes from the 2D hull (axis-aligned bounding box) of the projected corner points p_0, \dots, p_7 of a 3D-Treemap item:

$$a = |\max(p_{0x}, \dots, p_{7x})| - |\min(p_{0x}, \dots, p_{7x})|$$

$$b = |\max(p_{0y}, \dots, p_{7y})| - |\min(p_{0y}, \dots, p_{7y})|$$

For a given viewport resolution of w width and h height, we observed that $\epsilon \in [1, 2.5]$ the trade-off between performance improvement and visual artifacts seems optimal.

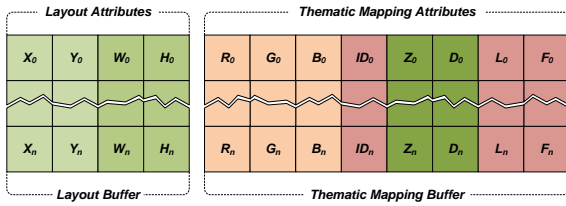


Figure 7: The Split-buffer concept for layout and thematic mapping information reduces update performance due to reduction of consumed bandwidth.

4 IMPLEMENTATION DETAILS

To evaluate and compare the performance of the rendering techniques described above, a prototypical implementation using OpenGL (Segal and Akeley, 2012) and GLSL is presented. The implementation uses modern GPU capabilities such as vertex buffer objects (VBO), vertex array objects (VAO), texture buffer objects (TBO), and uniform buffer objects (UBO). Assuming that the remaining techniques are well documented, this section focus on implementation details for the shape generation approach.

Buffer Management Based on the assumption that changes in thematic mapping occur more often than layout changes, we decided to use two buffer objects: one represents the 2D layout information (layout buffer) and the other represents the thematic mapping (thematic mapping buffer) information (Fig. 7). The buffer contents is organized in groups of four 32bit float values to support memory alignment constraints of the GPU. The split buffer implementation is only relevant for the shape generation, uniform-buffer as well as texture buffer instancing approaches.

Shape Generation using Shader For encoding the primitive template, one can use the approaches similar to encoding per-instance data (Section 3.4). We encode the primitive template using shader constant registers. Independent of the encoding, the size of the primitive template (e.g., the number of primitives represented) is effectively limited by the number of vertices and attributes that can be emitted by the geometry shader: 4096 float values.

The listing in Fig. 8 shows the OpenGL geometry shader implementation used for shape generation stage. The geometry template is encoded using constant shader registers for fast access. Shape generation is triggered only if the input point passes view-frustum and size culling performed in the previous vertex shader stage. The number of output vertices of the geometry shader is capped to 12.

```

in vec4 v4_Dimension_VS[1];
in float v1_Pass_VS[1];

const vec4 VERTEX[8] = vec4[](/* ... */);
const int INDEX[12] = int[](/* ... */);

void main(void){
    if(v1_Pass_VS[0] > 0.0){ // pass view-frustum & size culling
        vec4 VERTEX_TRANSFORM[8];
        for(int i = 0; i < 8; i++){ // Transform template vertices
            VERTEX_TRANSFORM[i] = gl_ModelViewProjectionsMatrix *
                (gl_PositionIn[0] + (VERTEX[i] * v4_Dimension_VS[0]));
        }
        for(int j = 0; j < 12; j++){ // Emit primitive
            gl_Position = VERTEX_TRANSFORM[INDEX[j]];
            EmitVertex();
        }
    }
}

```

Figure 8: GLSL geometry shader for the shape generation approach using shader constant registers to represent the primitive template.

The first loop scales each vertex of the template with respect to the dimension of the 3D-Treemap item. The scale vertex is then translated to the item origin and than projected. The compiled (unrolled) geometry shader requires only 120 assembly instructions for the respective geometry template.

3D-Treemap Stylization Suitable styling of 3D-Treemaps is essential for human perception. It should support the differentiation between single treemap items and facilitate the visual extraction of the treemap hierarchy. Stylization is implemented as a post-processing step in the rendering pipeline. Figure 9 shows an overview of the stylization stage and participated components. The G-Buffer (Saito and Takahashi, 1990) required for the deferred stylization are generated using render-to-texture (RTT) (Wynn, 2002) in combination with multiple rendering targets (MRT). The overhead in rendering performance introduced by RTT varies between 1-3 milliseconds on a NVIDIA GTX 560, depending on the screen resolution.

Figure 9 shows a comparison example for the used stylization variants, ordered by the impact on the rendering performance. Plain coloring and a single distance light (Fig. 9.A) performs best but makes it difficult for a user to differentiate between the treemap items (Bohnet and Döllner, 2011). This can be partially improved by implementing image-based edge-enhancement (Nienhaus and Döllner, 2003) (Fig. 9.2). For this stylization feature, per-face normal vectors are required. The normal vector information is not part of the treemap representation and generated procedurally using a geometry shader. For a triangle $T = (V_0, V_1, V_2)$ the normal N is simply computed by $N = normal(T) = |V_0 - V_1| \times |V_1 - V_2|$. For the shape generation approach the normal vectors are explicitly given for each emitted vertex using last provoking vertex (Segal and Akeley, 2012).

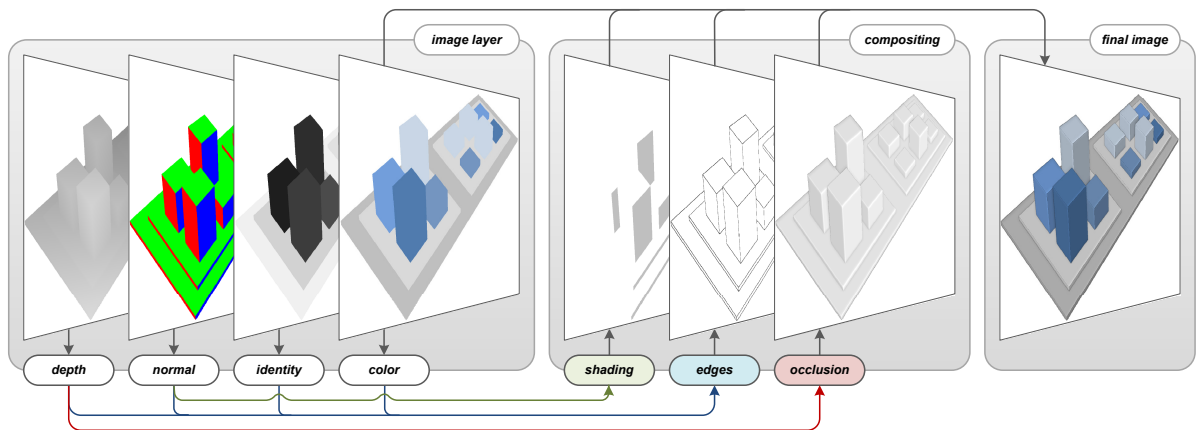


Figure 9: Image-based stylization pipeline used for all presented rendering techniques. The G-Buffer for depth, normal, identifier, and color, are rendered within a single using multiple render targets. The compositing stage use this data to synthesize various treemap stylization.

5 RESULTS & DISCUSSION

This section presents a comparative performance evaluation of the presented approach and discusses limitations and ideas for future work.

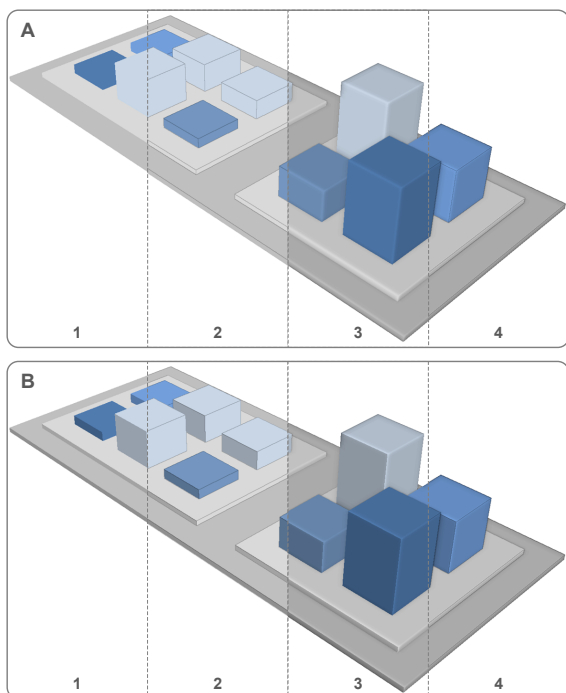


Figure 10: Various stylization alternatives supported by the stylization pipeline, without (A) and with static lighting (B). From left to right shows the item color only (1), applied edge-enhancement (2), unsharp masking (3), and unsharp masking combined with edge enhancement (4).

5.1 Test Setup

The rendering technique was tested using four data sets of different geometric complexity: 35.089, 96.658, 365.645, and 614.929 items. The performance tests are conducted on three different test platforms with different GPU generations: (1) NVIDIA GeForce GTX 460 GPU with 1024MB video memory on an Intel Xeon W3530 CPU with 2,8GHz and 6GB of main memory; (2) NVIDIA GeForce GTX 480 with 1.5GB video memory on an Intel Xeon W3520 2.67GHz and 24GB of main memory; and (3) NVIDIA GeForce GTX 560 Ti with 2GB video memory on an Intel Xeon W3550 3.07GHz and 6GB of main memory.

The test application runs in windowed mode at high-definition resolution of 1280×720 pixels. The complete scene is visible in the view frustum, thus view-frustum culling is not applied. Further back-face culling is activated and size culling is deactivated. For each rendering technique, a total of 5000 consecutive frames are rendered and the respective run-time performance in milliseconds is tracked. After performance tracking, all records are averaged. To determine to update performance, the time required between committing a new data set to the rendering techniques and the next frames rendered is measured in milliseconds. Styling is turned off to measure geometry throughput only with the RTT overhead.

5.2 Performance Evaluation

Figure 11 shows the results for the run-time performance evaluation for the novel shape generation (SG), pseudo instancing (PI), uniform-buffer instancing (UI), texture-buffer instancing (TI), index vertex

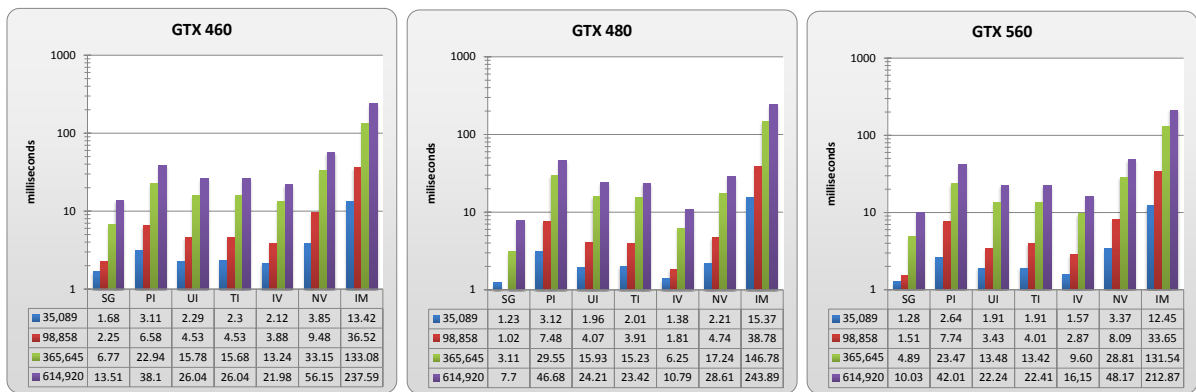


Figure 11: Comparison of the rendering performance for the presented rendering techniques on three different hardware platforms using four test datasets of varying complexity. The vertical axis shows the run-time performance in milliseconds on a logarithmic scale.

buffer (IV), non-indexed vertex buffer (NV), and intermediate approach (IM). Figure 12 shows the respective memory consumptions important for comparison. The visualized values are computed based on the functions presented in Table 1. The results show that the presented server-side shape generation approach outperforms the remaining rendering techniques on all tested hardware platforms. Indexed vertex- buffer rendering outperforms geometry instancing but comes at the cost of a larger memory footprint.

Uniform-buffer instancing outperforms pseudo- and texture-buffer instancing. In comparison to texture-buffer instancing, the number of required draw calls are higher, but the data access (L1 for uniform buffers) is faster (L2 for texture buffers). The performance of pseudo-instancing is CPU-bound because of the limited constant shader memory. The memory footprint the server-side 3D-Treemap representation of the instancing and shape generation are almost the same.

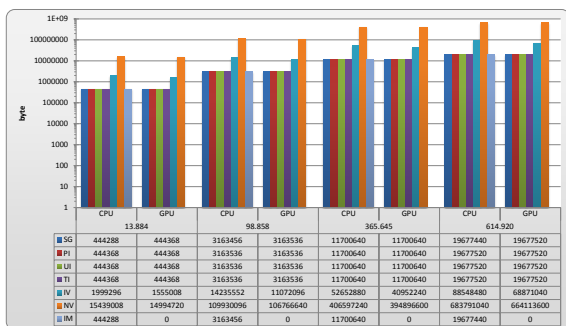


Figure 12: Memory footprint comparison of the presented rendering techniques using four test datasets. The vertical axis shows the amount of Bytes required for the client-(CPU) and server-side (GPU) representation of 3D-Treemaps using a logarithmic scale.

Rendering in intermediate mode do not require any video memory for the representation of a 3D-Treemap but is CPU-bound and thus performs worst. Non-indexed vertex buffer rendering performs worst of all rendering techniques using server side storage.

5.3 Discussion & Future Work

To summarize, if video memory is a limiting factor, shape generation and instancing approaches are preferable over vertex-buffer approaches. Based on the average run-time performance, the estimated theoretical number of 3D-Treemap items that can be rendered in real-time (assuming 12 frames-per-second) is approximately 5 millions.

However, the presented approach and its implementation has some conceptual and technical limitations. One major technical limitation concerns the encoding of the primitive template. Its geometrical complexity is limited to primitives and its attributes that can be represented using 4096 float values. (as described in Section 4).

Figure 13 shows a rendering of a complex 3D-Treemap. Due to static layout and border sizes, the perspective projection introduces cluttering and Moiré effects. Further, single 3D-Treemap items cannot be perceived anymore and complex 3D-Treemaps of the presented extends are hard to read and to interpret. To challenge these conceptual problems, some aspects of the treemap layout should be altered during rendering in a view-dependent or view adaptive way. This requires effective level-of-detail or level-of-abstraction approaches, which can be applied in real-time during rendering.

Although, the rendering techniques are not fill-limited, overdraw can be a further topic to address further performance increase (Sander et al., 2007).

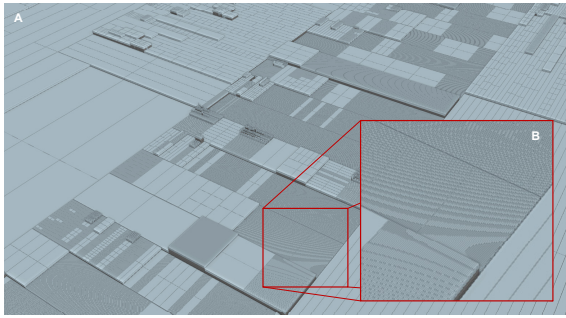


Figure 13: Problems for rendering of complex 3D-Treemaps: indistinguishable 3D-Treemap items (A) and Moiré effects (B) caused by perspective projection and high zoom levels.

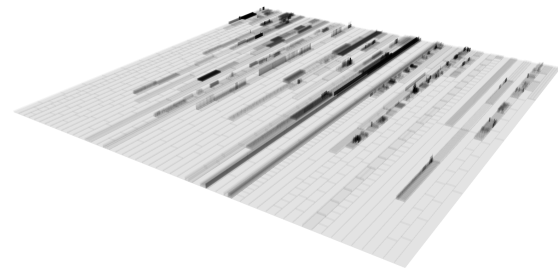


Figure 14: Visualization of overdraw for a 3D-Treemap of 35k items using a slice'n dice layout. Dark areas show high amount of overdraw (gamma-corrected).

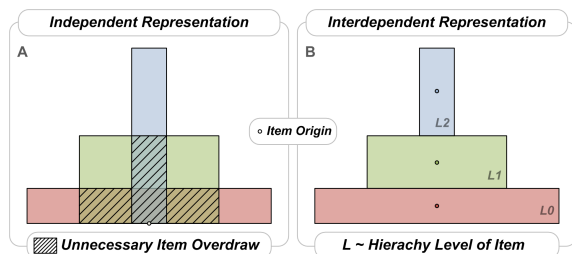


Figure 15: Side view for a possible approach to reduce unnecessary overdraw (A) by computing the the origin and dimension of a 3D-Treemap item based on its hierarchy level L (B).

The current data representation for the shape generation approach enables independent (height) scaling of each item but exhibit a relatively large amount of overdraw (Fig. 14). The average overdraw ratio of all rendered fragment to all visible fragments for a data set of 35k 3D-Treemap map items using a strip layout and oblique viewing of (Fig. 14) orientation are 96 percent, i.e., almost every pixel is overdrawn once. To reduce the overdraw ratio for possibly complex fragment processing, we strive for representing the

3D-Treemap item origin and dimensions based (currently Fig. 15.A) on a function of the level within the treemap hierarchy (Fig. 15.B).

For future work, we plan to focus on hardware accelerated implementation of treemap layout algorithms using parallel processors to enable true interactive 3D-Treemaps. We further strive towards a generalization of the rendering concept to support other types of 3D-Treemaps, such as 3D Voronoi treemaps (similar to (Choi et al., 2011)). Further, to deal for 3D tree maps with even higher geometric complexity, we plan to combine our approach with dynamic spatial data structures, such as the skip quad tree (Eppstein et al., 2005), and out-of-core rendering techniques. Furthermore, to increase the perception of complex 3D-Treemaps we research to what extent known level-of-detail (LoD) and level-of-abstraction (LoA) approaches (e.g., for the visualization of virtual 3D city models (Glander and Döllner, 2007)) can be transferred to the rendering and visualization of 3D-Treemaps.

6 CONCLUSIONS

This paper presents a novel rendering technique that enables real-time image synthesis of complex 3D-Treemaps. It can be completely implemented using consumer graphics hardware and outperforms existing rendering approaches. The presented technique is suitable for interaction metaphors that does not require to recompute the treemap layout. Further, it enables a compact, i.e., memory efficient, geometry representation of tree maps with large amount of items. Furthermore, a thoroughly performance evaluation and comparison is provided, that shows the superiority of the presented approach over existing rendering techniques.

ACKNOWLEDGMENTS

The authors would like to thank the anonymous reviewers for their valuable comments. This work was funded by the Federal Ministry of Education and Research (BMBF), Germany, within the InnoProfile Transfer research group "4DnD-Vis" (www.4dndvis.de) and the Research School on "Service-Oriented Systems Engineering" of the Hasso-Plattner-Institute.

REFERENCES

- Andrews, K., Wolte, J., and Pichler, M. (1997). Information pyramids (tm): A new approach to visualizing large hierarchies. In *Proceedings of the IEEE Visualization97*, pages 49–52.
- Balzer, M. and Deussen, O. (2005). Voronoi treemaps. In *Information Visualization, 2005. INFOVIS 2005. IEEE Symposium on*, pages 49–56. Ieee.
- Bao, G., Meng, W., Li, H., Liu, J., and Zhang, X. (2011). Hardware instancing for real-time realistic forest rendering. In *SIGGRAPH Asia 2011 Sketches, SA '11*, pages 16:1–16:2, New York, NY, USA. ACM.
- Bederson, B., Shneiderman, B., and Wattenberg, M. (2002). Ordered and quantum treemaps: Making effective use of 2d space to display hierarchies. *AcM Transactions on Graphics (TOG)*, 21(4):833–854.
- Bladh, T., Carr, D., and Kljun, M. (2005). The effect of animated transitions on user navigation in 3d tree-maps. In *Information Visualisation, 2005. Proceedings. Ninth International Conference on*, pages 297–305. IEEE.
- Bladh, T., Carr, D., and Scholl, J. (2004). Extending tree-maps to three dimensions: A comparative study. In *Computer Human Interaction*, pages 50–59. Springer.
- Bohnet, J. and Döllner, J. (2011). Monitoring code quality and development activity by software maps. In *Proceeding of the 2nd working on Managing technical debt*, pages 9–16. ACM.
- Bruls, M., Huizing, K., and Van Wijk, J. (2000). Squarified treemaps. In *Proceedings of the joint Eurographics and IEEE TCVG Symposium on Visualization*, pages 33–42. Citeseer.
- Choi, J., Kwon, O.-h., and Lee, K. (2011). Strata treemaps. In *ACM SIGGRAPH 2011 Posters, SIGGRAPH '11*, pages 87:1–87:1, New York, NY, USA. ACM.
- Correa, W., Klosowski, J., and Silva, C. (2003). Visibility-based prefetching for interactive out-of-core rendering. In *Proceedings of the 2003 IEEE Symposium on Parallel and Large-Data Visualization and Graphics*, page 2. IEEE Computer Society.
- Eppstein, D., Goodrich, M. T., and Sun, J. Z. (2005). The skip quadtree: a simple dynamic data structure for multidimensional data. In *Proceedings of the twenty-first annual symposium on Computational geometry, SCG '05*, pages 296–305, New York, NY, USA. ACM.
- Evans, F., Skiena, S., and Varshney, A. (1996). Optimizing triangle strips for fast rendering. In *Visualization'96. Proceedings.*, pages 319–326. IEEE.
- Fekete, J. and Plaisant, C. (2002). Interactive information visualization of a million items. In *Information Visualization, 2002. INFOVIS 2002. IEEE Symposium on*, pages 117–124. IEEE.
- Glander, T. and Döllner, J. (2007). Cell-based generalization of 3d building groups with outlier management. In *15th International Symposium on Advances in Geographic Information Systems (ACM GIS)*. ACM Press.
- Hoppe, H. (1999). Optimization of mesh locality for transparent vertex caching. In *Proceedings of the 26th annual conference on Computer graphics and interactive techniques, SIGGRAPH '99*, pages 269–276, New York, NY, USA. ACM Press/Addison-Wesley Publishing Co.
- Kong, N., Heer, J., and Agrawala, M. (2010). Perceptual guidelines for creating rectangular treemaps. *Visualization and Computer Graphics, IEEE Transactions on*, 16(6):990–998.
- Liggesmeyer, P., Heidrich, J., Münch, J., Kalcklösch, R., Barthel, H., and Zeckzer, D. (2009). Visualization of software and systems as support mechanism for integrated software project control. *Human-Computer Interaction. New Trends*, pages 846–855.
- Liktor, G. and Dachsbacher, C. (2012). Decoupled deferred shading for hardware rasterization. In *Proceedings of the ACM SIGGRAPH Symposium on Interactive 3D Graphics and Games, I3D '12*, pages 143–150, New York, NY, USA. ACM.
- Nguyen, H. (2007). *Gpu gems 3*. Addison-Wesley Professional, first edition.
- Nienhaus, M. and Döllner, J. (2003). Edge-enhancement - an algorithm for real-time non-photorealistic rendering. In *WSCG*.
- Rákos, D. (2010). Instance culling using geometry shaders. <http://rastergrid.com/blog/2010/02/instance-culling-using-geometry-shaders/>.
- Saito, T. and Takahashi, T. (1990). Comprehensible rendering of 3-d shapes. *SIGGRAPH Comput. Graph.*, 24(4):197–206.
- Sander, P. V., Nehab, D., and Barczak, J. (2007). Fast triangle reordering for vertex locality and reduced overdraw. *ACM Transactions on Graphics (Proc. SIGGRAPH)*, 26(3).
- Schulz, H., Hadlak, S., and Schumann, H. (2011). The design space of implicit hierarchy visualization: A survey. *Visualization and Computer Graphics, IEEE Transactions on*, (99):1–1.
- Schulz, H., Luboschik, M., and Schumann, H. (2007). Exploration of the 3d treemap design space. *Poster Compendium of IEEE InfoVis07*, pages 78–79.
- Segal, M. and Akeley, K. (2012). *The OpenGL Graphics System: A Specification (Version 4.2 (Core Profile) - April 27, 2012)*.
- Shneiderman, B. (1992). Tree visualization with tree-maps: 2-d space-filling approach. *ACM Transactions on graphics (TOG)*, 11(1):92–99.
- Sud, A., Fisher, D., and Lee, H. (2010). Fast dynamic voronoi treemaps. In *Voronoi Diagrams in Science and Engineering (ISVD), 2010 International Symposium on*, pages 85–94. IEEE.
- Wettel, R. and Lanza, M. (2008). Codecity: 3d visualization of large-scale software. In *Companion of the 30th international conference on Software engineering*, pages 921–922. ACM.
- Wynn, C. (2002). OpenGL Render-to-Texture. In *GDC*. NVIDIA Corporation.